Small-Angle Neutron Scattering Analysis of the Structure and Interaction of Triblock Copolymer Micelles in Aqueous Solution

Yingchun Liu,[†] Sow-Hsin Chen,*[,‡] and John S. Huang[§]

Department of Materials Science and Engineering and Department of Nuclear Engineering, 24−209, Massachusetts Institute of Technology, Cambridge, Massachusetts 02139, and Exxon Research and Engieering Company, Annandale, New Jersey 08801

Received August 19, 1997; Revised Manuscript Received January 3, 1998

ABSTRACT: We report analysis of an extensive set of small angle neutron scattering intensity distributions from triblock copolymer micelles in aqueous solutions. We investigated two Pluronics, P84 (PEO_{19} PPO_{43} PEO_{19}) and P104 (PEO_{27} PPO_{61} PEO_{27}), in an entire range of disordered spherical micellar phases both in temperature and in concentration. At room temperature, both poly(ethylene oxide) (PEO) and poly(propylene oxide) (PPO) are hydrophilic but at elevated temperature, PPO becomes significantly less hydrophilic, thus creating a thermodynamic driving force for micellization. It has been known that the resultant spherical micelle consists of a hydrophobic core and a hydrophilic corona region. In this paper, we propose a "cap-and-gown" model for the microstructure of the micelle, taking into consideration the polymer segmental distribution and water penetration profile in the core and corona regions. We take into account the intermicellar correlation using an adhesive hard sphere model of Baxter. With this combined model, we are able to fit satisfactorily all SANS intensities for the entire micellar range in an absolute scale. We obtain consistent trends for impotant parameters such as the aggregation number, hydration number per polymer in both the core and corona, and surface stickiness. The structure of micelle stays essentially constant as a function of concentration, but changes rapidly with temperature. Both the aggregation number and surface stickiness increase, and the micelle becomes drier with increasing temperature. The micellar core is not completely dry but contains up to 20% (volume fraction) of solvent molecules at lower temperatures.

I. Introduction

Self-assembling behavior of block copolymers in aqueous solution resembles the micelle formation of short chain surfactants with wider variations of molecular architecture and composition.[1] Poly(ethylene oxide) and poly(propylene oxide) containing block copolymers represent a class of polymers that associate spontaneously in aqueous solution. The self-association is characterized by sensitivity to the temperature and solvency.[2] In particular, many triblock copolymers composed of two symmetric poly(ethylene oxide)s and a poly(propylene oxide) have been synthesized as a class of polymeric surfactants.

Triblock copolymer surfactants we studied are commercially available under the tradename Pluronic from BASF.[3] They are ABA type block copolymers where the A blocks are poly(ethylene oxide)s and the B block is poly(propylene oxide). The total molecular weight and the composition, EO-to-PO ratio, of the block copolymer can be adjusted during the synthesis. The copolymer surfactants are water soluble to large weight percentages and in a broad temperature range. As hydrophobe modified copolymer surfactants, Pluronic polymer surfactants find widespread industrial applications in detergency, wetting, foaming/defoaming, emulsification, lubrication, and solublization, as well as in cosmetics, bioprocessing, and pharmaceutical applications.[3−5]

One of the most interesting features of the Pluronic polymer is its self-association in aqueous solutions and its resultant rich phase behavior.[4,6−13] At low polymer concentrations and low temperatures, the triblock copolymer in water exhibits single-coil behavior; such polymers are often called unimers. At higher concentrations or temperatures, the copolymer molecules self-associate to form thermodynamically stable aggregates—micelles. The micelles exist in a disordered phase within a wide temperature and concentration ranges. At even higher concentrations and temperatures, the copolymer chain and micelles can form ordered phases, such as cubic, hexagonal, and lamellar phases.[6,12,13] The self-assembly and phase behaviors of the copolymer solution depend on the total molecular weight and on the composition of the copolymer.

Micellization occurs above a certain critical micellization concentration and temperature (cmc and cmt). The cmc and cmt curves of the Pluronic surfactants have been studied extensively using various techniques.[7,8,14,15] Theoretical developments also allow systematic prediction of the unimer-to-micelle transition for a copolymer surfactant with given composition and molecular weight.[16−19] Micellizations have no sharp boundary but a rather broad coexistence region of large aggregates and single chained polymers. Dynamic light scattering shows that Pluronic micellar solutions exhibit significant polydispersity at low temperatures but become monodisperse at high temperatures.[7] Batch-to-batch variations of the surfactant supplies with composition heterogeneities, such as diblock copolymer impurities, may considerably affect micelle formation and surface tension but have little effect on the micellar structure and intermicellar interaction for concentrations beyond the cmc. We therefore limit our study on the microstructure and interaction of micelles far beyond micel-

[†] Department of Materials Science and Engineering, Massachusetts Institute of Technology.
[‡] Department of Nuclear Engineering, Massachusetts Institute of Technology.
[§] Exxon Research and Engineering Co.

S0024-9297(97)01253-9 CCC: $15.00
Published on Web 03/20/1998

lization boundaries and ignore such impurities and heterogeneities.

In this paper, we focus our attention on a particular Pluronic surfactant family, i.e., copolymers containing a 40−60 weight ratio of poly(ethylene oxide)s and poly(propylene oxide). This Pluronic family has several members, namely, P104, P94, P84, L64, and L44, with decreasing molecular weights. They all can self-associate into mesoscopic structures in aqueous solutions. Pluronic P104 and P84 with corresponding chemical formulas $PEO_{27}-PPO_{61}-PEO_{27}$ and $PEO_{19}-PPO_{43}-PEO_{19}$ are studied in detail. P84 and P104 have molecular weights of 4200 and 5900 and molecular volumes of 6920 and 9710 Å^3, respectively. The corresponding cloud points of their aqueous solutions are 75 and 85 °C, showing little concentration dependence. Among commercially available Pluronic surfactants with 40% EO, P104 has the highest and L44 has the lowest molecular weights. To clarify the effects of copolymer molecular weight, we also made some studies of the system made of L44 ($PEO_{10}-PPO_{23}-PEO_{10}$) for comparison, the results of which will not be reported here. Two of the 40% EO surfactants with intermediate molecular weights, P94 and L64, are neglected since their properties are believed to be between their neighbors.

To determine the range of the disordered micelle phase, it is important to measure its two boundaries, i.e., the micellization at low concentration and gelation at high concentration. The experimental cmc−cmt boundaries of the Pluronic P104, P84, and L44 in aqueous solutions are determined using light scattering method.[20] Micelles are formed as temperature or concentration increases beyond the cmc-cmt curves, corresponding to an abrupt increase of the scattering signals. The effect of molecular weight of the block copolymer on micellization is significant. For the surfactants with the same EO−PO composition, higher molecular weight polymer tend to form micelles at lower concentration and/or temperature.

Gelation of Pluronic solutions occurs at high polymer concentrations. For the 40% EO Pluronic family, the concentration of the sol−gel transition is only slightly dependent on temperature. The micellization and sol−gel transition are correlated: a higher cmc tends to correspond to a higher gelation concentration. However, the sol−gel boundary is nearly vertical on the phase diagram. For stable micellar solutions at temperature higher than 30 °C, the variation of gelation concentration is normally at most 1 or 2 wt % within a large temperature range. The gelation concentrations for Pluronic P104, P84, and L44 are 20, 22, and 24 wt %, respectively. It is clear that higher polymer molecular weight favors gelation. These gelation concentrations set the limit for the concentration ranges of the disordered micellar phases.

The aim of this paper is to investigate the microstructure and positional correlations of the polymeric micelles at concentrations far beyond the micellization boundary. Polymer concentration at the upper boundary of the disordered micellar phase is about 20 wt %. When the hydration effect of the copolymer is taken into account, the volume fraction of the micelles can be as high as 40 to 50%. The traditional methods in surface science, such as surface tension measurements, are useful in detecting the unimer-to-micelle transition boundary but are very limited in higher concentration dispersions. On the other hand, the scattering techniques have been proven to be powerful even at higher concentrations.[5,21,22] We have developed a practical method for analyzing absolute intensity data from SANS experiments. In general, the SANS intensity distribution function can be decomposed into an intraparticle structure factor and an interparticle structure factor. An explicit polymer segment distribution profile, called a cap-and-gown model, is proposed for the calculation of the intraparticle structure factor and an analytical expression for the interparticle structure factor based on an adhesive hard sphere model is given.

Mortensen[23] has previously given an alternative model of analysis for a micellar system formed by P85. This model is based on a core−shell structure of a micelle and a hard sphere intermicellar interaction. In our experience, if one takes a simple core−shell model of the micelle for the particle structure factor, one needs to introduce a considerable degree of polydispersity of size to fit the large k portion of the scattering intensity distribution. The advantage of our cap-and-gown model of the micellar structure to be described later is that we do not need to postulate a polydispersity to account for the large k data. Furthermore, we use a hard sphere with a surface adhesion to model the intermicellar interaction. This was shown previously to be a necessary ingredient to account for a substantial increase of zero shear viscosity as a function of temperature.[24]

II. Experiment

SANS experiments were performed at NIST using the 30-m SANS spectrometer (NG7). We used a wavelength λ of 7 Å with $\Delta\lambda/\lambda = 11\%$ at the sample to detector distances (SDD) of 2 m/15 m, covering a k (magnitude of the wave vector transfer) range of 0.001−0.230 Å^{-1}; and a λ of 5 Å at SDD of 1.3 m/10 m, covering a k range of 0.002−0.560 Å^{-1}. For all measurements, 1 mm spaced flat quartz cells were used. Samples were loaded to the scattering cells at room temperature, except for some concentrated samples, which were loaded at lower temperature. All samples appeared transparent and homogeneous. Samples were preheated in a separate water bath for hours before being moved to the spectrometer for SANS measurements. Temperature of the samples was controlled to an accuracy of 0.5 °C.

Pluronic polymer samples were obtained from BASF. The polymers were dissolved in deuterated water (Cambridge Isotopes) for SANS experiments without further purification or filtration. The same batch of polymer was used to carry out all experiments. Normally, a polymer solution was tested by using dynamic light scattering before SANS experiments were performed. The cmc−cmt curves obtained from dynamic light scattering served as a guideline for the concentration and temperature windows used in SANS measurements.

In SANS experiments we use deuterated water as the solvent to enhance the contrast between the micelle, which are made up largely of protonated polymers and some hydrated solvent molecules, and the solvent. The magnitudes of scattering length densities of the polymer segments and the solvent are illustrated in Figure 1 and their numerical values listed in Table 1.

III. Cap-and-Gown Model of Micellar Structure

We propose a new structural model which describes the polymer segment distribution and the solvent penetration profile in the polymeric micelle. This model combines both characteristic features of a diffuse distribution of polymer chains in the outer layer of the micelle and a global core−shell structure of the particle. Thus statistically we assume a uniform compact core but a Gaussian distribution of the polymer segments

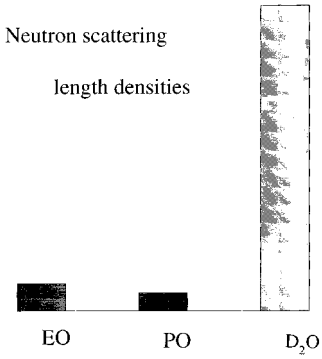

Figure 1. Neutron scattering length densities of the hydrogenated blocks of polymer PEO, PPO, and deuterated solvent D_2O. Note that neutron scattering length density of the deuterated solvent is very different from the polymer chains. This enhances the contrast.

Table 1. Molecular Volumes, Scattering Lengths and Scattering Length Densities of Polymer Surfactants and Solvent

species	chem formula	mol wt	mol vol (Å^3)	scale lengths $\sum b_i$ (fm)	scale length density (10^{-6} Å^2)
EO	$-(CH_2)_2O-$	44	72.4	4.14	0.572
PO	$-(CH_2)_3O-$	58	95.4	3.31	0.347
solvent	D_2O	20	30.3	19.153	6.321
P104	$PEO_{27}PPO_{61}PEO_{27}$	5900	9706	424.1	0.437
P84	$PEO_{19}PPO_{43}PEO_{19}$	4200	6920	302.1	0.437
L44	$PEO_{10}PPO_{23}PEO_{10}$	2200	3619	158.1	0.437

in the corona region, and therefore there is no abrupt boundary between the polymer chains and the solvent. The Gaussian distribution uses only one parameter to fully characterize the polymer segment density profile.

The inner core of the micelle is composed of mostly segments which are relatively incompatible with solvent molecules and thus likely to be more compact. The outer shell, on the other hand, accommodates polymer segments which are more compatible with the solvent and, therefore, adopts a less compact and more diffuse segmental distribution. A micelle formed by triblock copolymers of the PEO−PPO−PEO type in aqueous solution clearly exhibits a core of low polarity composed of mostly PPO blocks surrounded by a more polar region composed mostly of PEO blocks. The PEO blocks outside the core become more extended as the EO/PO ratio increases.

Figure 2 illustrates the cap-and-gown model of the micellar structure. The micellar core is described as the cap and the diffuse outer layer as the gown. The relative sizes of the cap and the gown are related by the PEO to PPO ratios. The figure shows the radial distribution of polymer segment volume fraction $\phi_p(r)$ in a micelle formed by Pluronic triblock copolymers with 40% PEO.

The radial segmental distribution in the core region starts out uniform within a radius a. It is joined to a Gaussian distribution with a width σ. Denoting by $\phi_w(r)$ the volume fraction occupied by solvent molecules at a radial distance r, the volume fraction occupied by the polymer segments $\phi_p(r)$ is then $1 - \phi_w(r)$. The cap-and-gown model assumes the water penetration profile to be

$$\phi_w(r) = \begin{cases} \phi_{core} & \text{for } 0 < r < a \\ 1 - \exp\left(-\dfrac{r^2}{\sigma^2}\right) & \text{for } a < r < \infty \end{cases} \quad (1)$$

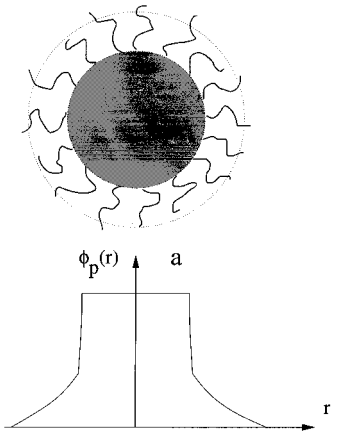

Figure 2. Schematic illustration of a cap-and-gown model for the radial distribution of polymer segment volume fraction in a micelle formed by Pluronic triblock copolymers with 40% PEO. The micellar core is described as the cap and the diffuse outer layer as the gown. The relative sizes of the cap and the gown are related by the PEO to PPO ratios. The water penetration profile is complementary to the polymer segment distrubution.

where r is the radial distance from the center of the core. Thus the polymer volume fraction is distributed as

$$\phi_p(r) = \begin{cases} \phi_p & \text{for } 0 < r < a \\ \exp\left(-\dfrac{r^2}{\sigma^2}\right) & \text{for } a < r < \infty \end{cases} \quad (2)$$

where the polymer segment volume fraction in the core is $\phi_p = 1 - \phi_{core}$.

The neutron scattering length density profile can be calculated in terms of the known scattering length densities of polymer, ρ_p, and water, ρ_w, as

$$\rho(r) = \phi_w(r)\rho_w + \phi_p(r)\rho_p \quad (3)$$

The difference between the scattering length density of polymers and that of solvent (the contrast) determines the particle structure factor

$$\Delta\rho(r) = \rho(r) - \rho_w = [\rho_p - \rho_w]\phi_p(r) \quad (4)$$

The core radius a, the Gaussian width σ and the polymer volume fraction in the core ϕ_p are related by a geometrical constraint. We assume that all PPO blocks reside in the core and PEO chains are distributed outside the core as a Gaussian. We note that this assumption does not in practice imply a complete segregation of the PPO and PEO distributions. Since scattering length densities and mass densities of PEO and PPO blocks are very close, replacing some PPO segments by the same volume of PEO segments causes little change in the overall scattering length density profile. Thus the model allows the interdiffusion of PEO and PPO segments for the reason that the exchange hardly affects the scattering length density profile of the micelle.

The total volume of polymer segments in the core, V_p^{in}, is related to the aggregation number N and the PPO segments volume in a polymer chain by

$$V_p^{in} = \frac{4\pi}{3}a^3\phi_p = N v_{PPO} \quad (5)$$

Table 2. Ratios of Core Radius to Gaussian Width for Pluronic Micelles with Different Compositions, Assuming No Solvent Penetration Inside the Core, i.e., $\phi_p = 1$

PEO wt %	v_{PEO}/v_{PPO}	$t = a/\sigma$	σ/a	$\exp(-t^2)$
10	0.11	1.438	0.695	0.13
20	0.25	1.253	0.798	0.21
30	0.43	1.130	0.885	0.28
40	0.67	1.030	0.971	0.35
50	1.00	0.937	1.067	0.42
60	1.50	0.845	1.183	0.49
70	2.33	0.744	1.343	0.57
80	4.00	0.622	1.608	0.68

Similarly, the total volume of polymer segments outside the core, V_p^{out} is

$$V_p^{out} = 4\pi \int_a^\infty \exp\left(-\frac{x^2}{\sigma^2}\right) x^2 \, dx = N v_{PEO} \qquad (6)$$

We define the ratio of the core radius a to the Gaussian width σ as $t \equiv a/\sigma$. From the above two equations the polymer volumes in and out of the core are related by

$$\frac{v_{PEO}}{v_{PPO}} = \frac{3\int_t^\infty \exp(-x^2)x^2 \, dx}{t^3 \phi_p} \qquad (7)$$

Simplifying the right-hand side of the above equation, we can obtain the ratio t by solving the following nonlinear equation

$$\frac{\exp(-t^2)}{t^2} + \frac{\sqrt{\pi}}{2t^3}\mathrm{erfc}(t) = \frac{2}{3}\phi_p \frac{v_{PEO}}{v_{PPO}} \qquad (8)$$

where erfc(x) is the complementary error function. The right-hand side of the above equation contains the known block polymer composition ratio and thus gives a relation between t and ϕ_p. Table 1 gives the relevant molecular parameters of the Pluronics with various A−B ratios.

As an example, for the first approximation, one may set $\phi_p = 1$, assuming no solvent penetration in the core. For Pluronic with 40% PEO content, the right-hand side of the above equation equals 0.444. Solving the nonlinear equation, we have $t = 1.03$. Thus for Pluronic P104, P84, and L44 the core radius-to-Gaussian width ratio is approximately unity. As the fractional PEO composition of the copolymer increases, the t value would decrease, resulting in more extended chains outside the core. For example, the a/σ ratio for 60 wt % PEO is 0.85. Table 2 lists the ratios a/σ and σ/a for Pluronics with PEO weight percent ranging from 10 to 80.

The cap-and-gown model of the polymer segmental distribution proposed here is qualitatively consistent with theoretical predictions.[18] It captures the most important feature in the overall segmental distribution and is simple enough to allow an analytical evaluation of the particle structure factor. A merit of the cap-and-gown model is that it describes the complex distribution of the copolymer segments without introducing many parameters. For a given copolymer composition, the core radius a and the Gaussian width σ are known once the aggregation number N is known, assuming no water penetration in the core. If the water volume fraction inside the core increases from zero, the core radius and a/σ ratio will increase accordingly. Thus higher water penetration in the core has the similar effects as lower hydrophile-hydrophobe ratio, v_{PEO}/v_{PPO}, of the block copolymer. This makes possible a way to determine the water penetration inside the core by SANS data analysis.

To calculate the particle structure factor, one needs to do a Fourier transform of the neutron scattering length density radial distribution

$$F(k) = \int \Delta\rho(r) \exp(i\vec{k}\cdot\vec{r}) \, d^3r = \frac{4\pi a^2}{k}(\rho_p - \rho_w)[\phi_p j_1(ka) + \int_1^\infty \exp(-t^2x^2)\sin(kax)x \, dx] \qquad (9)$$

It is more convenient to define a normalized form factor by dividing $F(k)$ by its $k = 0$ value

$$F(0) = (\rho_p - \rho_w)\frac{4\pi a^3 \phi_p}{3}\left(1 + \frac{v_{PEO}}{v_{PPO}}\right) \qquad (10)$$

It is straightforward to show that

$$F(0) = \int \rho(r) \, d^3r - \rho_w \int d^3r = \sum_{micelle} b_i - V_{micelle}\rho_w = N(\sum_i b_i - \rho_w v_m) \qquad (11)$$

The scattering function at zero momentum transfer contains the scattering lengths and volume of the dry (nonhydrated) polymer. Thus the normalized form factor $\tilde{F}(k)$ is given by

$$F(k) = N(\sum_i b_i - \rho_w v_m)\tilde{F}(k)$$

$$\tilde{F}(k) = \frac{v_{PPO}}{v_{PEO} + v_{PPO}}\left[\frac{3j_1(ka)}{ka} + \frac{3}{\phi_p}\int_1^\infty \frac{\sin(kax)}{ka}\exp(-t^2x^2)x \, dx\right] \qquad (12)$$

The normalized particle structure factor is $\tilde{P}(k) = |\tilde{F}(k)|^2$.

The normalized form factor of the cap-and-gown model may be considered equivalent to that of polydisperse spheres where the boundaries are smeared by a distribution. Determination of the details of the microstructure depends on the micellar compositions and is ultimately limited by the experimental k resolution. The details of the micellar structure cannot be determined by SANS to a dimension smaller than neutron wavelength without ambiguity. It is likely that the boundary of the micellar core is also diffuse rather than sharp, and the distribution of polymer segments outside the core may deviate from the Gaussian form. As far as SANS data analysis is concerned, a spatial deviation of the scattering length density profile within a few angstroms is hard to distinguish. The adequacy of the microstructure modeling can ultimately be checked by the quality of the fits to SANS data.

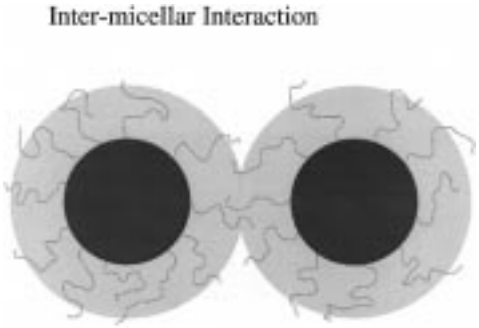

Figure 3. Schematic illustration of intermicellar interaction. The micellar core is composed of mostly polymer segments, shown as the dark region. The gray region outside the core contains polymer segments and most of the hydrated water molecules. At the micellar interface, there is a region of interpenetrating polymer chains. The intermicellar interaction is described by a hard sphere repulsion, which represents the excluded volume effect, together with a surface adhesion.

IV. Intermicellar Interaction and the Structure Factor

The most important micelle−micelle interaction comes from the excluded volume effect. Volume fraction of the micelles ϕ characterizes the strength of the interaction. To a first approximation, micelles can be regarded as hard spheres. Micelles are, however, swollen by solvent molecules, mostly in the corona region. Polymer chains and the hydrated water molecules both contribute to the excluded volume. The intermicellar distance is comparable with micellar diameter at high volume fractions. The real volume of a micelle is significantly larger than the volume of the dry polymer chains alone. It is the real volume of the micelle rather than the polymer volume that determines thermodynamical quantities such as the osmotic compressibility and scattering intensities. Obtaining the real volume of a micelle in a self-consistent way is nontrivial. It requires a knowledge of the detailed microstructure such as hydration number per polymer chain. This information on the associated solvent molecules has not been available from theoretical predictions and is hard to extract accurately from scattering intensities at dilute concentrations. For a more accurate description, polymeric micelles cannot be regaded simply as the smooth-surfaced hard spheres because of possible additional interaction at their surface.

The origin of the surface adhesion is the interpenetration of polymer chains and the depletion effect of solvent molecules. When two micelles come into contact, there is an overlapping region where polymer chains can interpenetrate, squeezing out some solvent molecules. In the penetrated region, the intermicellar interaction is an averaged effect of the delicate balance of interactions between the polar, nonpolar polymer segments and water molecules from one micelle with those from the other micelle. In particular, the interaction between the nonpolar segments may contribute most significantly. The interpenetration gives rise to an effective attraction at the micellar surface in addition to the excluded volume repulsion. This effect is illustrated by Figure 3.

Interparticle Structure Factor of an Adhesive Hard Sphere Model

The interparticle structure factor of a system of interacting spheres is determined by the interparticle interaction potential $u(r)$. The relation between the direct correlation function $c(r)$ and the net correlation function $h(r)$ is expressed by an Ornstein−Zernike (OZ) equation[25]

$$h(r) = c(r) + \rho\int \mathrm{d}\vec{r}'\, c(r')h(|\vec{r} - \vec{r}'|) \qquad (13)$$

where ρ is the particle number density. The net correlation function $h(r)$ is related to the radial distribution function $g(r)$ by $h(r) = g(r) - 1$. For given ρ, T, and $u(r)$, the OZ equation may be solved under a Percus−Yevick approximation[26] for the functions $g(r)$, $h(r)$, and $c(r)$.

We consider a system of hard spheres with adhesive surface. The pairwise interparticle interaction potential is written as

$$\frac{u(r)}{k_{\mathrm{B}}T} = \begin{cases} \infty & \text{for } 0 < r < R' \\ -\Omega & \text{for } R' < r < R \\ 0 & \text{for } R < r \end{cases} \qquad (14)$$

where $R - R'$ is the thickness of the adhesive surface layer. Baxter[27] considered solution of the OZ equation in the PY approximation in the limit that the thickness of the adhesive layer goes to zero but the adhesive potential Ω tends to infinity in such a way that one can introduce a finite stickiness parameter $1/\tau$ defined as $1/\tau = 12\exp(\Omega)(R - R')/R$.[28] The second virial coefficient of the system in this limit has a simple expression in terms of the stickiness $1/\tau$. Baxter used the PY approximation to solve the OZ equation to the first order in the fractional surface layer thickness $\epsilon = (R - R')/R$. The solution is expressed in terms of the following set of parameters for a given volume fraction ϕ (defined in terms of the inner diameter R' of the hard sphere) and the stickiness $1/\tau$

$$\Gamma = \frac{\phi(1 + \phi/2)}{3(1 - \phi)^2} \qquad (15)$$

$$\Delta = \tau + \frac{\phi}{1 - \phi} \qquad (16)$$

$$\lambda = \frac{6(\Delta - \sqrt{\Delta^2 - \Gamma})}{\phi} \qquad (17)$$

$$\mu = \lambda\phi(1 - \phi) \qquad (18)$$

$$\alpha = \frac{(1 + 2\phi - \mu)^2}{(1 - \phi)^4} \qquad (19)$$

$$\beta = -\frac{3\phi(2 + \phi)^2 - 2\mu(1 + 7\phi + \phi^2) + \mu^2(2 + \phi)}{2(1 - \phi)^4} \qquad (20)$$

We use a dimensionless parameter $Q \equiv kR$, the product of the magnitude of the wavevector transfer k and the outer particle diameter R. The interparticle structure factor $S(Q)$ of the sticky hard sphere system ($\epsilon \to 0$, $\Omega \to \infty$ in such a way that $1/\tau = 12\exp(\Omega)\epsilon$ remains finite) is then given analytically as[24]

$$\frac{1}{S(Q)} - 1 = 24\phi\left[\alpha f_2(Q) + \beta f_3(Q) + \frac{1}{2}\alpha\phi f_5(Q)\right] + \phi^2\lambda^2 f_1(Q) - 2\phi\lambda f_0(Q) \qquad (21)$$

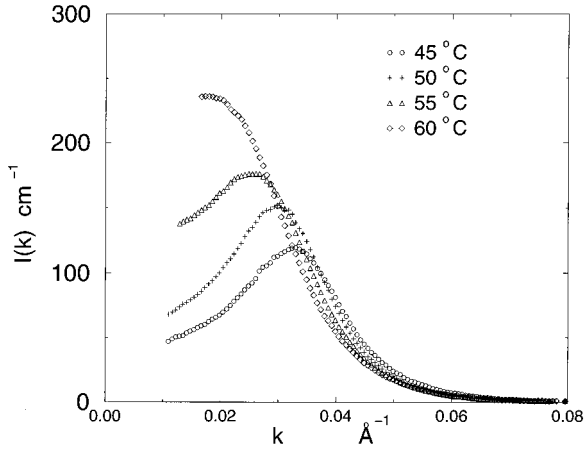

Figure 4. SANS intensity distribution functions of a 10% Pluronic P104 in deuterated water show the temperature effect of the self-association of the micelles by triblock copolymer. At higher temperatures, scattering intensities increase, and peak positions shift toward smaller k, due to increasing aggregation numbers. The enhanced self-association is a consequence of increased hydrophobicity of the polymer segments at high temperature.

where various functions are defined as $f_0(x) = \sin(x)/x$; $f_1(x) = (1 - \cos(x))/x^2$; $f_2(x) = (\sin(x) - x\cos(x))/x^3$; $f_3(x) = (2x\sin(x) - (x^2 - 2)\cos(x) - 2)/x$;[4] $f_5(x) = (4x^3 - 24x)\sin(x) - (x^4 - 12x^2 + 24)\cos(x) + 24)/x$.[6] The hard sphere limit is obtained by setting $1/\tau \rightarrow 0$ and $\lambda \rightarrow 0$.

V. SANS Data Analysis

The absolute scattering intensity $I(k)$ (in a unit of cm^{-1}) is proportional to the product of the normalized particle structure factor $\tilde{P}(k)$ and the interparticle structure factor $S(k)$, with a proportionality factor which consists of the polymer concentration c (number of polymer molecules per milliliter), the aggregation number of a micelle N, and the contrast factor square.[29] In the contrast factor within the square bracket, the first term is the sum of coherent scattering lengths of atoms comprising of a polymer molecule, ρ_w the scattering length density of the solvent and v_m the polymer molecular volume.

$$I(k) = cN[\sum_i b_i - \rho_w v_m]^2 \tilde{P}(k) S(k) \qquad (22)$$

It is important to note that the absolute intensity is directly proportional to the aggregation number N. The polymer concentration and the contrast factor are known quantities. Figure 4 illustrares the temperature effect on the scatering intensity. The figure shows clear evidence that the micelle grows as temperature increases.

In our model, the fitting parameters are the aggregation number N, the total hydration number H (no. of water molecules attached to a polymer in a micelle), stickiness $1/\tau$, outer micellar diameter R, and polymer volume fraction in the core ϕ_p. Other parameters, such as the volume fraction of micelles ϕ, core radius a, Gaussian distribution width σ, and the hydration numbers in the core and shell, are deduced quantities. The more sensitive parameters of the fit are the aggregation number N, the total hydration number H, and the micellar diameter R. The aggregation number determines the overall amplitude of the scattering intensity and can be obtained by fitting SANS data in an absolute intensity scale. The total hydration number determines the volume fraction of micelles which controls the peak height of the structure factor $S(k)$. The micellar diameter determines the peak position of $S(k)$. These three parameters basically decide the general shape and amplitude of $I(k)$. Two less sensitive parameters determine the detailed rise and fall of the scattering peak and small and large k behaviors of the scattering intensity. These parameters are the stickiness and the polymer volume fraction in the core.

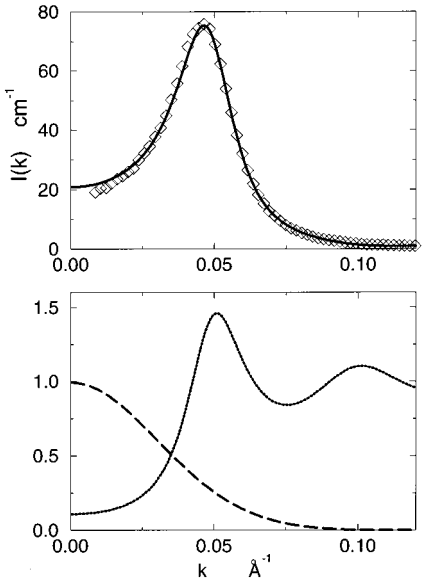

Figure 5. SANS intensity distribution and its model fit (solid line) as decomposed into the inter- and intra- particle structure factors $S(k)$ and $P(k)$ for a 16% Pluronic P84 solution in D_2O at 40 °C. The interparticle structure factor is calculated by solving the OZ equation with an intermicellar potential of an adhesive hard sphere system. The intraparticle structure factor is calculated using the cap-and-gown model as the polymer segment distribution in a micelle.

A Fortran code based on a gradient searching nonlinear least-squares fitting method[30] was written and used to fit SANS intensities in an absolute scale. The quality of the fits is uniformly excellent for systems of spherical micelles in the entire range of the disordered micellar phase. As an illustation, the calculated particle structure factor, interparticle structure factor and the absolute intensity distribution for a typical fit to an intensity distribution is shown in Figure 5.

Parameters characterizing the microstructure and interaction of P84 and P104 polymeric micelles thus obtained are listed in the following tables. To show consistency of the fits, a set of concentration series at a constant temperature and their fits are shown in Figure 6.

We find that at a given temperature, the ratio of the volume fraction of micelles to the volume fraction of dry surfactant molecules is a constant. Furthermore the stickiness parameter is also a constant. This leads us to conclude that, in contrast to a typical ionic micellar solution, the microstructure of micelles formed by triblock copolymers of PEO and PPO is determined only by temperature, independent of the polymer concentration.

The overall aggregation number of the polymeric micelles is around 100, similar to the values for micelles formed by short chain surfactants. The aggregation number increases with temperature. In the intermediate temperature range, the number of associated sur-

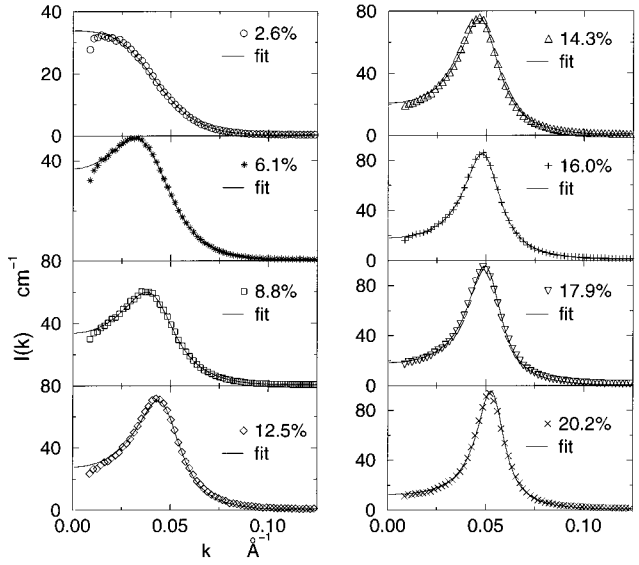

Figure 6. Series of SANS data and their fits for Pluronic P84 micellar solutions at 40 °C. The fits in absolute intensity scale use an adhesive hard sphere model for the interparticle structure factor and a cap-and-gown model for the form factor. The same stickiness and polymer segment distribution are used to fit the entire series of SANS data in this graph simutaneously by varying only the polymer concentrations. This indicates that the microstructure of self-associated micelles is independent of the polymer concentration.

factant molecules increases almost linearly with temperature and the number density of the micelles decreases accordingly. At a given polymer concentration, micelles grow and become less populated in the solution. The outer micellar radius remains more or less the same (differs by maximum 10%) in all cases. This agrees with the results of similar micellar solutions studied by other researchers.[19] The core size of the micelles increases, but the diameter keeps unchanged with temperature. This suggests that the micelles carry less solvent molecules and become more compact at higher temperatures.

It is also found that the number of bound solvent molecules is independent of polymer concentration at a given temperature. The hydration number decreases with temperature as the micelles become more compact at high temperatures. The hydrated water molecules take up a large fraction of volume in a micelle. For example, for Pluronic P84 micelle at intermediate temperatures, the hydration number for each polymer chain is 240. Knowing the specific volume of a water molecle (30 Å^3) and the molecular volume of P84 (6920 Å^3), we obtain the volume ratio of hydrated water to polymer in a P84 micelle to be about 1.05. This means that more than 50% of the micellar volume is occupied by the solvent molecules. The effect of hydration thus contributes significantly to the properties of the micellar solution. This number is hard to obtain from theoretical models for polymer segment distribution. However, with a proper liquid theory, it can be extracted from the SANS intensity profile of a concentrated micellar solution. SANS analysis also gives the stickiness parameter. The stickiness of micellar surface indicates that at low temperature,the micelles are close to hard spheres. The surface of the micelles become stickier as micelles grow at elevated temperatures. This effect is consistent with increased hydrophobicity of the polymers at elevated temperatures.

A water penetration profile gives an interesting result. The micelle has regions of core and shell with distinctly different polymer and solvent volume fractions. The core of a Pluronic micelle is not completely dry, in agreement with theoretical predictions.[18] The polymer volume fraction in the core is about 92−97% at higher temperatures, independent of temperature and concentration. This suggests that only at most 8% of volume inside the core is occupied by the solvent. However, at low temperatures, the water penetration seems to depend on the concentration. For P84 at 35 °C, the polymer volume fraction in the core goes from 80% at concentration of 2.6 wt % up to 96% at concentration of 18 wt %. It can be concluded that, at high

Table 3. Parameters of the Microstructure and Interaction of P84 Polymeric Micelles at 35 °C Extracted from SANS Experiments

concn (wt %)	aggregation N	hydration H	$1/\tau$	diameter R (Å)	ϕ_p	core radius a (Å)	micelle ϕ
2.6	45	220	0.10	120	0.80	39	0.06
6.1	44	235	0.14	118	0.82	39	0.13
8.8	44	236	0.13	123	0.87	38	0.18
12.5	44	241	0.15	125	0.87	38	0.28
17.9	45	239	0.15	122	0.96	37	0.37

Table 4. Parameters of the Microstructure and Interaction of P84 Polymeric Micelles at 40 °C Extracted from SANS Experiments

concn (wt %)	aggregation N	hydration H	$1/\tau$	diameter R (Å)	ϕ_p	core radius a (Å)	micelle ϕ
6.1	52	201	0.28	130	0.94	39	0.13
8.8	53	220	0.26	133	0.93	38	0.19
12.5	54	212	0.27	129	0.96	38	0.26
14.3	55	216	0.24	128	0.97	38	0.30
16.0	51	206	0.29	127	0.96	37	0.33
17.9	54	211	0.25	127	0.95	37	0.35
20.2	52	198	0.27	126	0.97	37	0.40

Table 5. Parameters of the Microstructure and Interaction of P84 Polymeric Micelles at 45 °C Extracted from SANS Experiments

concn (wt %)	aggregation N	hydration H	$1/\tau$	diameter R (Å)	ϕ_p	core radius a (Å)	micelle ϕ
2.6	66	191	0.38	130	0.92	41	0.05
6.1	66	195	0.34	135	0.95	41	0.11
8.8	64	189	0.37	136	0.96	40	0.16
12.5	65	192	0.36	135	0.96	40	0.22
17.9	66	200	0.38	134	0.95	40	0.32

Table 6. Parameters of the Microstructure and Interaction of P84 Polymeric Micelles at 55 °C Extracted from SANS Experiments

concn (wt %)	aggregation N	hydration H	$1/\tau$	diameter R (Å)	ϕ_p	core radius a (Å)	micelle ϕ
2.6	81	142	0.48	145	0.93	44	0.05
6.1	80	126	0.47	145	0.95	44	0.10
8.8	80	134	0.45	146	0.94	43	0.15
12.5	79	130	0.43	146	0.96	43	0.21
17.9	78	129	0.47	142	0.95	43	0.29

Table 7. Parameters of the Microstructure and Interaction of P104 Polymeric Micelles at 45 °C Extracted from SANS Experiments

concn (wt %)	aggregation N	hydration H	$1/\tau$	diameter R (Å)	ϕ_p	core radius a (Å)	micelle ϕ
4.2	85	484	0.1	173	0.94	52	0.12
6.6	85	478	0.1	172	0.93	51	0.18
10	84	475	0.1	170	0.95	51	0.29

Table 8. Parameters of the Microstructure and Interaction of P104 Polymeric Micelles at 50 °C Extracted from SANS Experiments

concn (wt %)	aggregation N	hydration H	$1/\tau$	diameter R (Å)	ϕ_p	core radius a (Å)	micelle ϕ
4.2	105	425	0.29	182	0.94	54	0.10
6.6	102	435	0.26	183	0.96	54	0.15
10	106	439	0.27	180	0.95	54	0.25

Table 9. Parameters of the Microstructure and Interaction of P104 Polymeric Micelles at 55 °C Extracted from SANS Experiments

concn (wt %)	aggregation N	hydration H	$1/\tau$	diameter R (Å)	ϕ_p	core radius a (Å)	micelle ϕ
4.2	121	360	0.50	191	0.94	56	0.11
6.6	119	365	0.46	196	0.96	56	0.13
10	120	355	0.50	190	0.95	56	0.28

Table 10. Parameters of the Microstructure and Interaction of P84 Polymeric Micelles Extracted from SANS Intensities

temp (°C)	aggregation N	hydration H	core radius a (nm)	diameter R (nm)	$1/\tau$
35	44	240	3.7	10.5	0.1
40	54	210	3.8	10.8	0.25
45	66	190	4.0	11.5	0.35
55	80	130	4.3	11.8	0.45

Table 11. Parameters of the Microstructure and Interaction of P104 Polymeric Micelles Extracted from SANS Intensities

temp (°C)	aggregation N	hydration H	core radius a (nm)	diameter R (nm)	$1/\tau$
45	85	480	5.2	15.8	0.1
50	105	430	5.4	17.0	0.28
55	120	360	5.6	17.3	0.50

temperatures, a polymeric micelle formed by Pluronic triblock copolymers becomes more compact. It has a larger association number but smaller hydration number.

The total molecular weight of a polymer has a profound influence on the micellization. Polymeric micelles formed by Pluronic surfactants with different molecular weights have different microstructures. Parameters of the microstructure and interactions of P84 and P104 micelles are listed in Table 10 and Table 11 as a function of temperature.

SANS analysis shows that at higher temperatures, diameters of P84 and P104 micelles are roughly 120 and 180 Å respectively. The aggregation number of P104 is higher than that of P84. This is consistent with the lower cmc−cmt curve for a higher molecular weight surfactant. From the hydration number for Pluronic P104 at intermediate temperatures, the average ratio of hydrated solvent volume to polymer volume is about 1.5. The overall polymer volume fraction in a P104 micelle is about 40%. This means that polymeric micelles formed with P104 are more hydrated than those formed with the P84 polymer. Micelles formed by a polymer with higher molecular weight tend to have a higher aggregation number and carry a larger amount of solvent molecules. This study suggests a way to control total micelle volume fraction in solution by varying the molecular weight of the triblock copolymer.

VI. Conclusion

We have demonstrated that the cap-and-gown model for polymer segmental distribution inside a micelle coupled with the adhesive hard sphere model for the intermicellar interaction gives a satisfactory description of the structure and thermodynamics of miceller systems made of of Pluronic polymers in aqueous solution. One can also achieve a moderately good fit to the scattering intensity distribution by using an uniform core−shell model for the particle structure factor, but in this case one needs to introduce a substantial polydispersity of sizes. The cap-and-gown model has an advantage that by having a diffuse scattering length density distribution in the shell region, one can achieve a satisfactory fit to the intensity at large k without introducing a polydispersity. We find that as temperature increases, the pure hard sphere interaction is no longer sufficient to account for the intermicellar interaction. Certain amount of attraction between micelles is needed. The correct level of hydration plays a vital role in giving the right volume fraction of the micellar system without which the excluded volume effect can never be properly accounted for. One important feature of a self-assembled system is that the mesoscopic scale structure of the particle depends in an essential way on the thermodynamic state of the solution. In this work we are able to achieve a quantitative understanding of the coupling of the two in a consistent way.

Acknowledgment. This research is supported by a grant to S.H.C. from the Materials Chemistry Division

of US DOE. Y.C.L. is grateful for fellowship supports from Exxon Research and Engineering Co. and Texaco Research Center. SANS measurements were made with the NG7 Small Angle Station at NIST.

References and Notes

(1) Tuzar, Z.; Kratochvil, P. *Surf. Colloid Sci.* **1993**, *15*, 1.
(2) Lindman, B.; Carlsson, A.; Karlstrom, G.; Malmsten, M. *Adv. Colloid Interface Sci.* **1990**, *32*, 183.
(3) *Pluronic and Technical Brochure Tetronic Surfactants*; BASF Corp.: Parsipanny, NJ, 1989.
(4) Alexandridis, P.; Hatton, T. A. *Colloids Surf.* **1995**, *96*, 1.
(5) Chu, B. *Langmuir* **1995**, *11*, 414.
(6) Wanka, G.; Hoffmann, H.; Ulbricht, W. *Macromolecules* **1994**, *27*, 4145.
(7) Zhou, Z.; Chu, B. *J. Colloid Interfacial Sci.* **1988**, *126*, 171.
(8) Brown, W.; Schillen, K.; Almgren, M.; Hvidt, S.; Bahadur, P. *J. Phys. Chem.* **1991**, *95*, 1850.
(9) Schillen, K.; Brown, W.; Johnsen, R. M. *Macromolecules* **1994**, *27*, 4825.
(10) Mortensen, K. *Prog. Colloid Polym. Sci.* **1993**, *91*, 69.
(11) Almgren, M.; Alsins, J.; Bahadur, P. *Langmuir* **1991**, *7*, 446.
(12) Almgren, M.; Brown, W.; Hvidt, S. *Colloid Polym. Sci.* **1995**, *273*, 2.
(13) Mortensen, K.; Brown, W.; Jorgensen, E. *Macromolecules* **1994**, *27*, 5654.
(14) Alexandridis, P.; Athanassiou, V.; Fukuda, S.; Hatton, T. A. *Langmuir* **1994**, *10*, 2604.
(15) Grieser, F.; Drummond, C. J. *J. Phys. Chem.* **1988**, *92*, 5580.
(16) Karlstrom. *J. Phys. Chem.* **1985**, *89*, 4962.
(17) Linse, P.; Malmsten, M. *Macromolecules* **1992**, *25*, 5434.
(18) Linse, P. *Macromolecules* **1994**, *27*, 2685.
(19) Hurter, P. N.; Scheutjens, J. M. H. M.; Hatton, T. A. *Macromolecules* **1993**, *21*, 5592.
(20) Liu, Y. C. Microstructure of micelles formed by triblock copolymer in water; relation to rheology of solutions. Ph.D. Thesis, MIT, March, 1997.
(21) Mortensen, K.; Schwahn, D.; Jansen, S. *Phys. Rev. Lett.* **1993**, *71*, 1728.
(22) Mortensen, K.; Pedersen, J. S. *Macromolecules* **1993**, *26*, 805.
(23) Mortensen, K. *J. Phys.: Condens. Matt.* **1996**, *8*, A103−A124.
(24) Liu, Y. C.; Chen, S. H.; Huang, J. S. *Phys. Rev. E* **1996**, *54*, 1698.
(25) Ornstein, L. S.; Zernike, F. *Proc. Acad. Sci., Amsterdam* **1914**, *17*, 793.
(26) Percus, J. K.; Yevick, G. J. *Phys. Rev.* **1958**, *110*, 1.
(27) Baxter, R. J. *J. Chem. Phys.* **1968**, *49*, 2770.
(28) Ku, C. Y.; Chen, S. H.; Rouch, J.; Tartaglia, P. *Int. J. Thermophys.* **1995**, *16*, 1119.
(29) Kotlarchyk, M.; Chen, S. H. *J. Chem. Phys.* **1983**, *79*, 2461.
(30) Bevington, P. R. *Data Reduction and Error Analysis for the Physical Sciences*; McGraw-Hill: New York, 1969.

MA971253O